Ultrastructural, Cytochemical, and Immunocytochemical Study of Nuclei and Cytoskeleton of Thyroid Papillary Carcinoma Cells

Olga M. Echeverría, PhD

Laboratory of Electron Microscopy, Faculty of Sciences, National Autonomous University of México (U.N.A.M.), México D. F., México

Rogelio Hernández-Pando, MD, PhD

Department of Pathology, National Institute of Nutrition, México D. F., México

Gerardo H. Vázquez-Nin, PhD

Laboratory of Electron Microscopy, Faculty of Sciences, National Autonomous University of México (U.N.A.M.), México D. F., México

One of the most constant and typical histological markers of thyroid papillary carcinoma is the presence of multilobated and ground-glass nuclei. With the intention of extending and characterizing the ultrastructural comprehension of this feature, thyroid papillary carcinoma cells and normal follicular cells were studied using chromatin and ribonucleoprotein preferential staining techniques, as well as immunolabeling with antibodies against DNA, lamins, vimentin, and desmin. Carcinoma cells showed scant compact chromatin arranged in small masses. A special type of nuclear bodies with DNA immunoreactive fibrils was found in these cells. Some nucleoli were surrounded by a double fibrillar layer limiting a perinucleolar space occupied by RNP fibrogranular structures that differed from those of normal nuclei. Perichromatin granules were scarce compared to normal follicular cells. Immunoelectron microscopic studies of lamins showed diminished immunoreactivity in the nuclei of carcinoma cells. A perinuclear distribution of desmin and vimentin filament was found in tumor cells. The cytoplasm of normal follicular cells showed scarce immunoreactivity to vimentin and no immunolabeling for desmin. Both types of filaments attach to the nuclear pore complex and to other regions of the nuclear envelope. Contacts between labeled filaments and desmosomes or hemidesmosomes were frequent. The results show that in papillary thyroid carcinoma cells, changes in the distribution of chromatin and ribonucleoproteins, either alone or in conjunction with scarce lamin immunolabeling and perinuclear vimentin and desmin filamentous rings, may be responsible for the characteristic ground glass and multilobated nuclei.

Keywords *intermediate filaments, lamin, nuclear bodies, RNP*

Papillary carcinoma is the most common malignant neoplasm of the thyroid gland [1]. Its classical histological features are fine papillae with central fibrovascular stalks covered by overlapping columnar tumor cells with ground-glass nuclei, with or without psammoma bodies [2–4]. The nuclei are round or slightly oval. Close inspection of thin sections and particularly electron microscopy reveal nuclear membrane irregularities in the form of folds or indentations, which may produce pseudoinclusions or grooves [5–7]. The former arise from deep cytoplasmic invaginations and result in acidophillic inclusion-like structures that compress and marginate the chromatin. The nuclear grooves are more common in oval-shaped nuclei. They are deep and slender invaginations, usually parallel to the long axis of the nuclei [7]. Another characteristic feature of the nuclei is an empty appearance. These nuclei seem almost totally devoid of chromatin strands, though ultrastructural examination reveals finely dispersed chromatin [8]. These nuclei are larger than normal follicular epithelial cells and have been described as pale, clear, ground glass, or watery. The optically clear nucleus has been recognized as an important histological feature of papillary carcinoma of the thyroid, and is now considered a diagnostic marker as important as the papillae [7, 8].

The nuclear envelope invaginations of papillary carcinoma cells may result from a defect of nuclear skeletal or cytoskeleton proteins. In fact, the inner face of the nuclear envelope is normally associated with a mesh of a special class of intermediate filaments (IF) called lamins [24]. The lamins constitute the nuclear lamina, which is an important support of the nuclear membrane. In this function cytoplasmic IF like vimentin, among others, can be also important. Indeed, cytoskeleton proteins like vimentin normally form a delicate network of thread-like filaments surrounding the nucleus and extending through the

Received November 17, 1997; Accepted February 18, 1998.
The authors are indebted to R. Benavente for providing L3f4 antibody and helpful comments. We thank S. Juárez Chavero for photographic work.
Address correspondence to: Dr. Gerardo H. Vázquez Nin, Lab. de Microscopía Electrónica, Facultad de Ciencias, U.N.A.M., Apartado postal 70-438, México D. F., México. E-mail: ghvn@hp.fciencias.unam.mx

0191-3123/98 $12.00 + .00

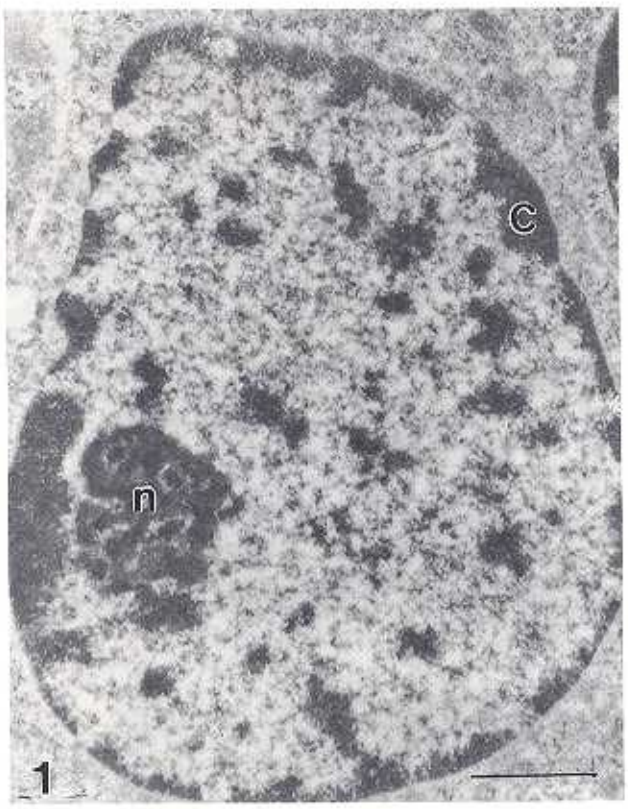
C
n
1

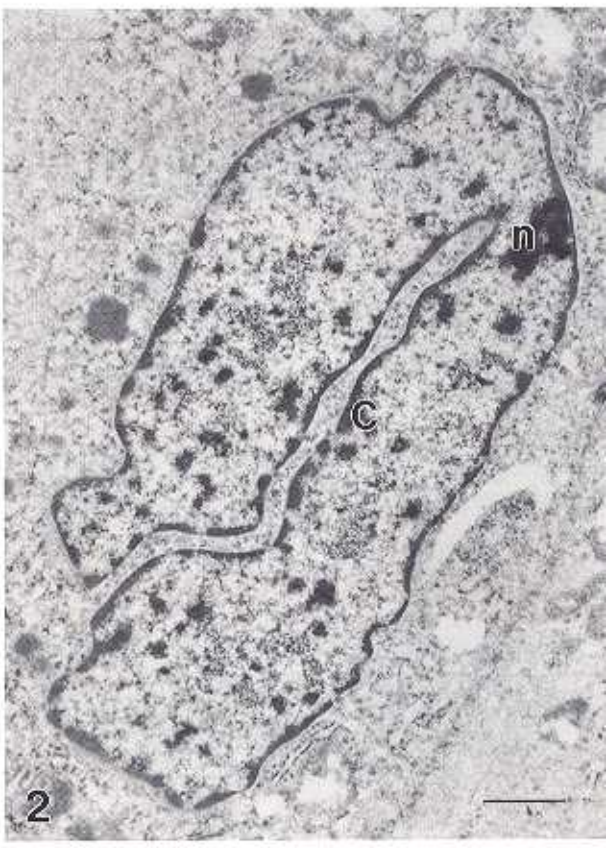
n
C
2

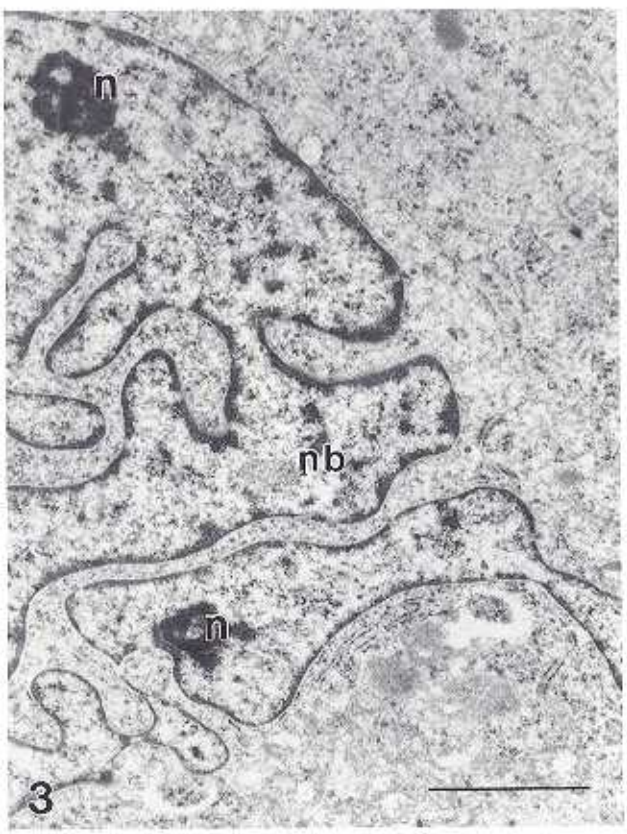
n
nb
n
3

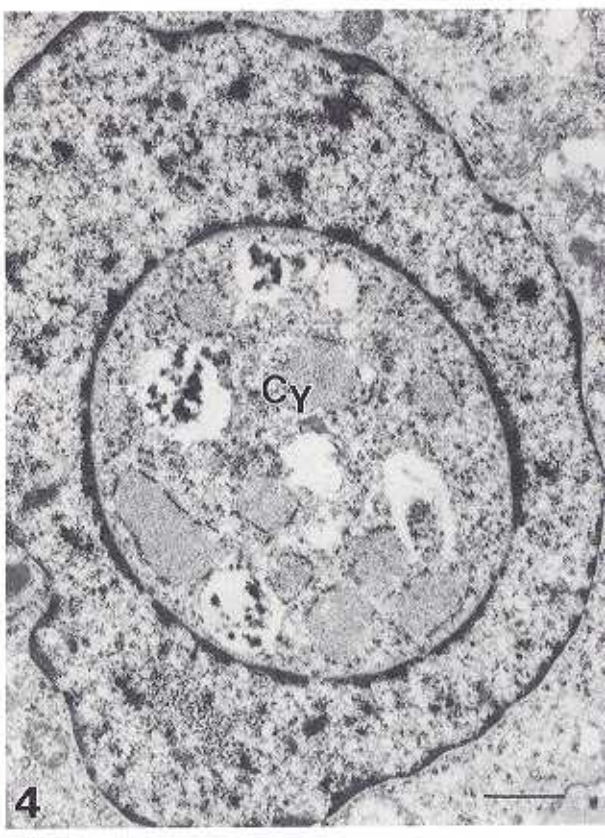
Cy
4

cytoplasm, where in some places they are collinear with cytoplasmic microtubule [25]. This suggests that many cytoplasmic IFs may be linked to the nuclear envelope and that they are normally pulled outward toward the cell periphery by attachment to microtubule or cell membrane.

The nonnucleolar ribonucleoproteic (RNP) component of the mammalian interphase nucleus, perichromatin fibrils, perichromatin granules, and interchromatin fibrils and granules, were characterized by Monneron and Bernhard [9]. Since these pioneer findings, numerous investigations have been carried out trying to relate these particles to the known functions of the nucleus [9—11]. Now it is known that the perichromatin fibrils contain pre-mRNA undergoing splicing [12–15]. Perichromatin granules (PCG) are involved in storage of processed mRNA [16, 17]. Interchromatin granules are mainly composed of low molecular weight RNAs rich in uridine (snURNA) and their associated proteins. They are related to the pre-mRNA splicing [14]. The frequency and distribution of these RNP structures exhibit important variations during embryonic development [21, 22], changes in hormone concentration [18–20], and neoplastic transformation [23].

The cell nucleus of papillary thyroid carcinoma has a very peculiar morphology, which may be due to abnormalities in the chromatin, RNPs, nuclear lamina, and/or cytoplasmic IF. To investigate which structures could account for the presence of multilobated and ground-glass nuclei in the neoplastic cells, we studied the interphase nucleus and cytoplasm of normal follicular cells and papillary thyroid carcinoma cells with electron microscopy, using preferential contrast techniques for chromatin and RNPs, as well as immunoelectron microscopy to locate DNA and intermediate filaments of the nuclear lamina (lamins) and cytoskeleton (vimentin and desmin).

MATERIALS AND METHODS

Five papillary thyroid carcinomas were removed surgically, fixed in 10% formaldehyde, and embedded in paraffin wax for light microscopy examination. Sections were stained with hematoxylin/eosin. Small fragments were fixed in 2.5% glutaraldehyde in 0.16 M phosphate buffer at pH 7.3 for 2 h at room temperature. Then, the samples from each case were divided into two groups: Half were dehydrated in alcohol and embedded in Epon for conventional transmission electron microscopy study. The other half were dehydrated and embedded in LR white. Sections were stained with the uranyl acetate–EDTA–lead citrate technique preferential for RNP-containing structures, and with the phosphotungstic acid method (PTA) preferential for chromatin, according to the procedures previously published [26, 27]. For immunoelectron microscopy, tumor and normal tissue fragments were immediately fixed in 4% paraformaldehyde dissolved in Sörensen buffer, pH 7.4, for 2 h at 4°C. After rinsing, free aldehyde groups were blocked in 0.5 M ammonium chloride in PBS for 1 h. Tissue fragments were dehydrated in graded ethyl alcohol and embedded in L-R white.

Sections 70 to 90 nm thick were placed on nickel grids. One of the following mouse monoclonal antibodies was used as first antibody in indirect immunolocalizations: anti-DNA (IgM) (Progen), antihuman vimentin (IgG) (Dako), antihuman desmin (IgG) (Dako), or L3f4 anti-rat lamins IgM [28]. The grids were incubated overnight at 4°C with a 1/20 solution of the antibody in PBS with 1% of bovine serum albumin (BSA) and 0.5% of Tween-20. After being rinsed with PBS, the grids were incubated for 1 h at room temperature with rabbit anti-mouse IgG conjugated to 10- to 15-nm gold particles diluted 1/50 in PBS. Finally, the grids were contrasted with uranyl salts and lead citrate and examined in the electron microscope. To get a better resolution of nuclear lamins, some grids were digested with RNAse and DNAse before the incubation with its specific monoclonal antibody.

RESULTS

Nuclear Ultrastructure of the Normal Follicular Cell and the Papillary Carcinoma Cell

The nucleus of the normal follicular cell is round to oval, usually with one small eccentric nucleolus and chromatin clumped in masses (Figure 1). In contrast,

FIG. 1 *Normal thyroid follicular cell nucleus stained with uranyl acetate and lead citrate. It is oval in shape with no indentations. Compact chromatin* (c) *appears as a discontinuous layer in contact with nuclear envelope and scattered clumps in nucleoplasm. The nucleolus* (n) *presents a nucleolonemal structure. Bar* = 1 μm, ×17,500.

FIG. 2 *Nucleus of a papillary carcinoma cell stained as in Figure 1. Its normal shape is altered by a profound indentation. The nucleolus* (n) *is small. The peripheral layer of compact chromatin* (c) *is thin but nucleoplasmic clumps are abundant. Bar* = 1 μm, ×11,000.

FIG. 3 *Nucleus of a papillary carcinoma cell stained as in Figure 1. Indentations are numerous and so profound that the nucleus appears lobated. The peripheral layer of compact chromatin is very thin and the nucleoplasmic clumps are small and less frequent than in the nucleus in Figure 2. n, small nucleoli; nb, nuclear body. Bar* = 1 μm, ×22,500.

FIG. 4 *Nucleus of a papillary carcinoma cell stained as in Figure 1. A large invagination of cytoplasm* (Cy) *is seen inside the nucleus* (pseudoinclusion). *Bar* = 1 μm, ×11,300.

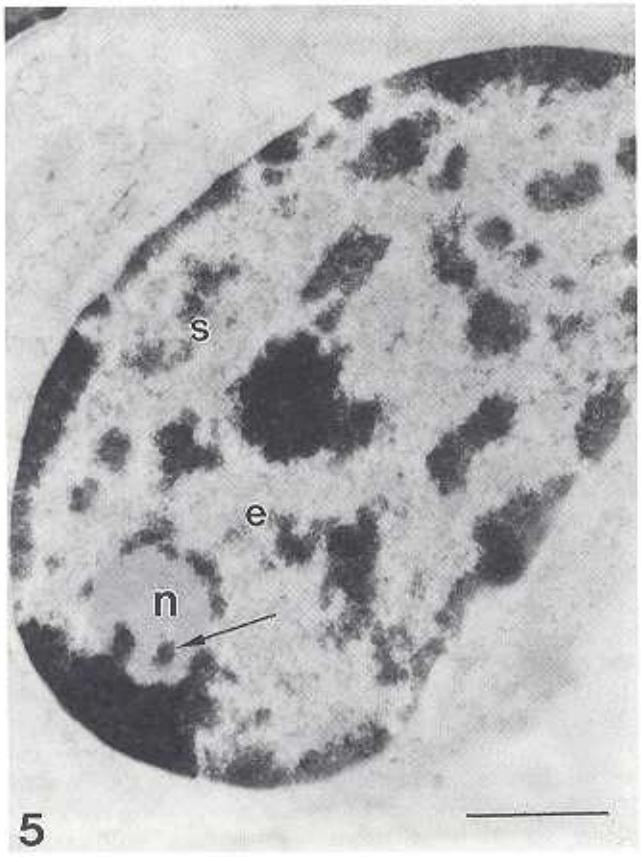

5

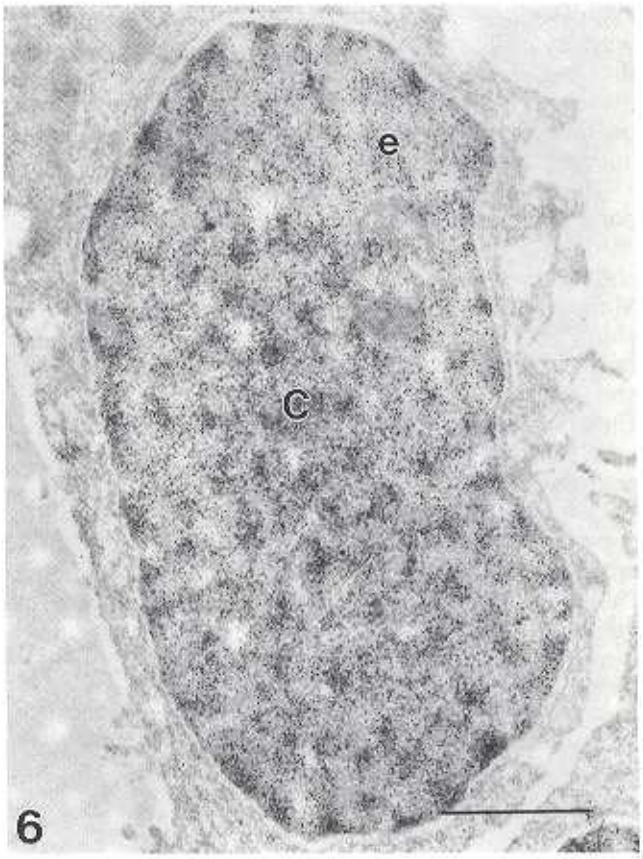

6

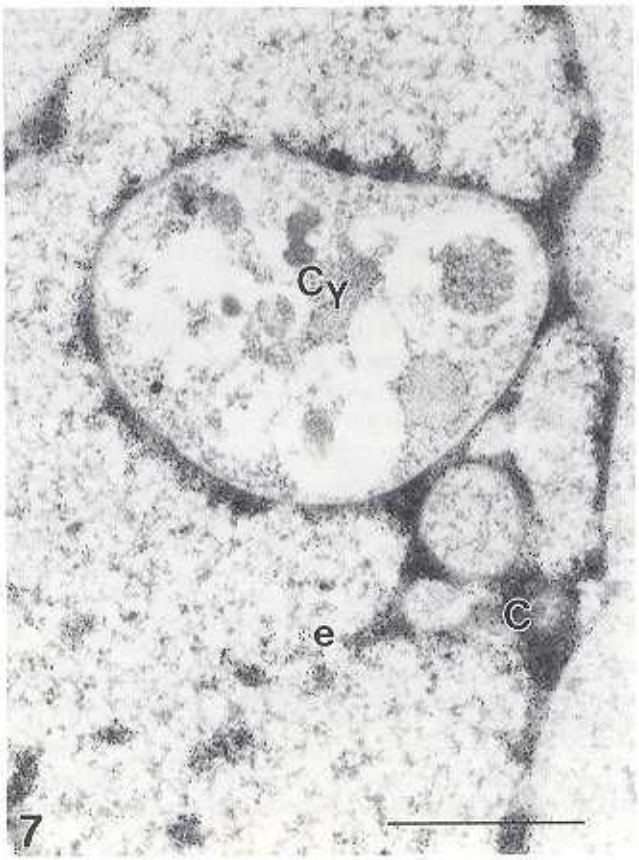

7

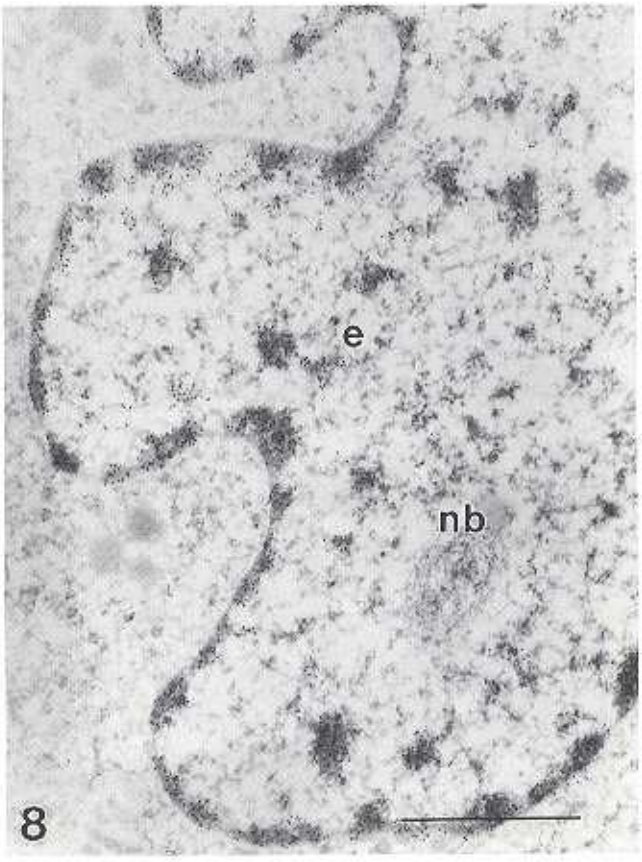

8

the papillary carcinoma cell nuclei are polymorphic. Some show deep and narrow indentations (Figure 2) or exhibit multiple invaginations of the nuclear envelope (Figure 3) with cytoplasmic pseudoinclusions that contain segregated cytoplasmic organelles (Figure 4). Nucleoli are numerous, present a dense nucleolonemal network, and are frequently apposed to the nuclear envelope (Figures 2, 3). Much of the nucleolar polymorphism is due to important differences in the development of the granular component.

Ultrastructural Cytochemistry and Immunocytochemistry of Chromatin- and RNP-Containing Structures

In normal follicular cells the PTA preferential staining procedure demonstrates that compact chromatin usually forms a thick discontinuous layer in contact with nuclear envelope and occurs as granules in the nucleoplasm (Figure 5). The pattern of distribution and the abundance of compact chromatin present ample variations that probably correspond to the different cytophysiological states of the follicular cells. Less frequently the nucleus of normal follicular cells contains abundant extended chromatin and numerous small clumps of compact chromatin in contact with the nuclear envelope and scattered in the nucleoplasm, as shown in Figure 6 by DNA immunolocalization.

Compact chromatin is frequently scant in the polymorphic nuclei of the cells of papillary carcinoma (Figures 7, 8). It is distributed in a thin peripheral layer, usually about 0.1 μm thick and in fine nucleoplasmic granules 0.1 to 0.2 μm in diameter (Figure 7), or in a diffuse arrangement of small masses surrounded by semicompact chromatin and a large network of extended chromatin (Figure 8).

Perichromatin granules are frequent in normal cells with abundant compact chromatin, as can be seen in sections stained using the EDTA procedure preferential for RNP-containing structures (Figure 9). Cancer cells with deformed nuclei usually contain few perichromatin granules and scarce compact chromatin. However, important changes in the frequency of these granules can be see, probably related to the ample variation of cytophysiological states and degrees of differentiation present in the population of cancer cells (Figures 10, 11).

A thin layer of filaments surrounding the nucleolus as a hollow sphere is frequently seen in nuclei of papillary carcinoma cells. One or two layers of filaments are extended in circles. The halo of 150–350 nm between the nucleolus and the spherical sheet of filaments is occupied by irregular radial fibrogranular structures that contact the fibrous layer and/or the nucleolus. Both fibrillar and granular components of the nucleolus may show direct continuities with these radial EDTA positive fibrogranular structures. This layer and the intervening region constitute an exclusion zone of masses of compact chromatin and standard RNP-containing particles as perichromatin granules and interchromatin granules and fibers (Figure 12).

Nuclear bodies of types 1, 2, and 3 [29] are frequent in nuclei of papillary carcinoma cells (Figures 3, 8, 10). The filaments contained in the nuclear bodies of type 1 or 2 are not stained with EDTA. In contrast, the small granules of the nuclear bodies type 2 are darkly stained with this method for RNPs (Figure 10). Large spherical nuclear bodies of peculiar structure and composition are present in nuclei of thyroid cancer cells. They are composed of three layers: (1) an external layer formed by fine fibrils faintly stained by uranyl acetate and lead citrate and loosely distributed; (2) an intermediate layer of densely arranged darkly stained fibrils; and (3) an internal layer of well-stained thick fibrils, loosely arranged. The dark-stained fibrils of the intermediate layer show an intense immunoreactivity to anti-DNA monoclonal antibody (Figure 13).

Immunoelectron Microscopy of Nuclear and Cytoplasmic Intermediate Filaments

Normal follicular cells showed scarce immunolabeling for vimentin and no immunoreactivity to

FIG. 5 *Normal follicular cell nucleus stained with phosphotungstic acid. Compact chromatin is arranged in a discontinuous peripheral layer and large clumps in the nucleoplasm. The unstained nucleolus* (n) *is partially surrounded by clumps of compact chromatin. The arrow points to intranucleolar compact chromatin. Semicompact* (s) *and extended* (e) *chromatin are also seen. Bar* = 1 μm, ×19,000.

FIG. 6 *Nucleus of a normal follicular cell faintly stained with uranyl acetate and lead citrate to highlight the gold grains of the anti-DNA labeling. Compact chromatin* (c) *is distributed in peripheral and nucleoplasmic small clumps. A large amount of extended chromatin* (e) *is localized by this procedure. Bar* = 1 μm, ×20,000.

FIG. 7 *Nucleus of a carcinoma cell stained with uranyl acetate and lead citrate. Compact chromatin* (c) *is labeled by anti-DNA Mab. Moderate amounts of extended chromatin* (e) *are decorated with gold grains. Cy, cytoplasmic pseudoinclusion. Bar* = 1 μm, ×26,000.

FIG. 8 *Nucleus of a carcinoma cell stained with uranyl acetate and lead citrate. A thin peripheral layer of compact chromatin and small nucleoplasmic clumps are labeled by anti-DNA Mab. Sparse filaments of extended chromatin* (e) *are also labeled. The nuclear body* (nb) *is devoid of gold grains. Bar* = 1 μm, ×24,000.

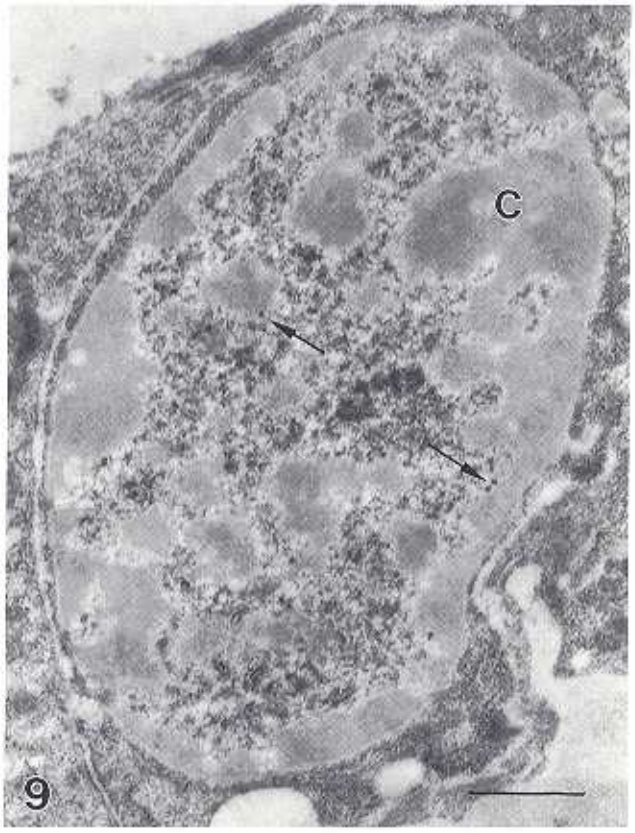
C
9

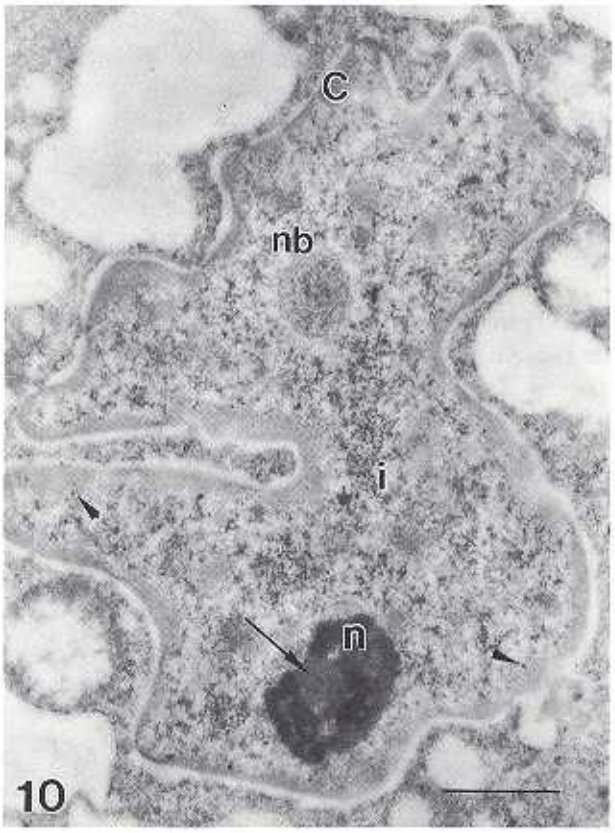
C
nb
i
n
10

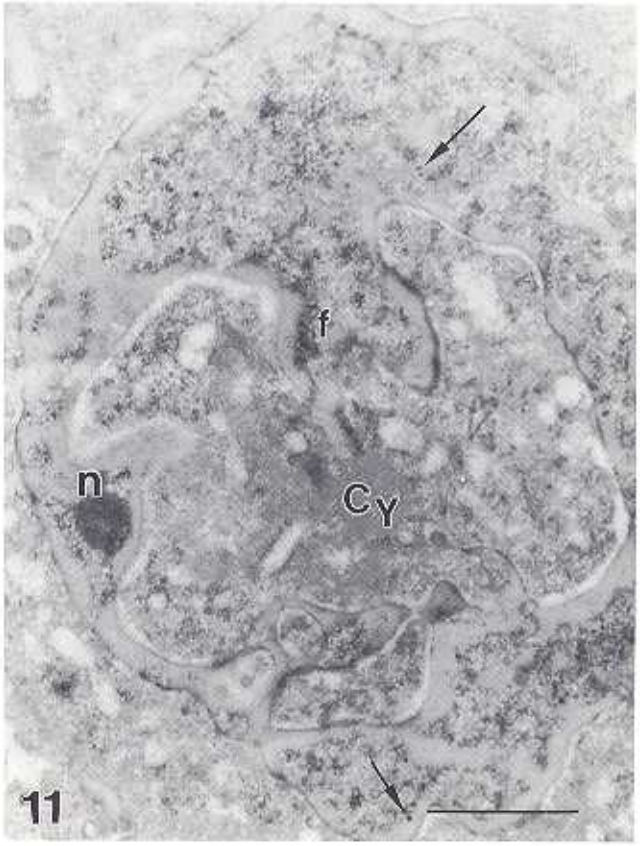
f
n
Cy
11

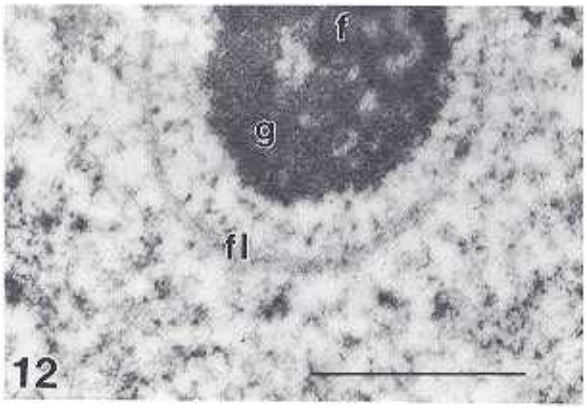
f
g
fl
12

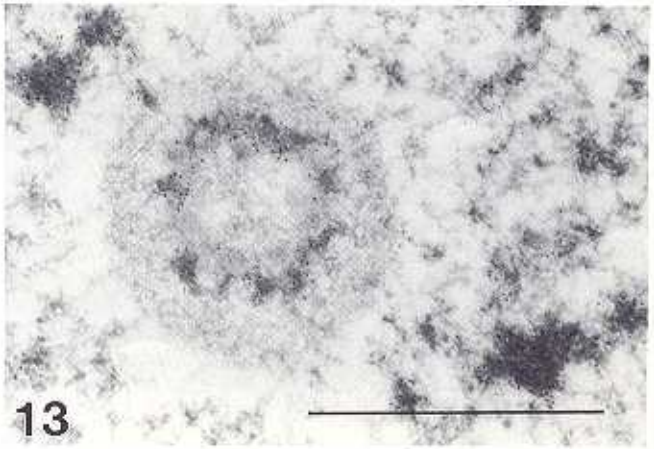
13

desmin. In contrast, tumor cells with indented nuclei have large bundles of filaments extending around the nucleus roughly parallel to the nuclear envelope (Figures 14–16) or stretching toward the cell membrane (Figures 17, 18). These filaments are continuous with a peripheral network of filaments heavily labeled by anti-vimentin or anti-desmin antibodies. Insertions of filaments in the cell membrane are frequently seen. Some of them attach to dense plaques corresponding to desmosomes (Figure 19) and hemidesmosomes (Figure 20), but more frequently the attachments are mediated by thin, scattered, dense regions (Figures 19, 20). Some filaments insert in the nuclear envelope by means of filaments associated with the pore complex (Figure 15) or in other regions of the envelope (Figures 16, 18). All these filaments are intensely immunolabeled by the monoclonal antibody against vimentin (Figures 14–16, 18, 20) and desmin (Figures 17, 19).

The nuclei of normal follicular cells usually show abundant lamin immunolabeling. Interestingly, numerous gold grains are present in the nucleoplasm and around compact chromatin, in addition to those labeling the lamina (Figure 21). In contrast, lobated and ovoid nuclei of papillary carcinoma cells showed mild lamin immunolabeling (Figure 22).

DISCUSSION

Our ultrastructural findings confirm and extend the classical descriptions of papillary thyroid carcinoma at the ultrastructural level [5, 6]. With regard to the nuclear structure, many tumor cells showed slender and deep indentations or multilobation with cytoplasmic pseudoinclusions. Morphological and cytochemical staining procedures, as well as DNA immunolocalization, showed that most of cancer cells present much less compact chromatin than normal cells. Some cancer cells contain small amounts of compact chromatin distributed in clumps of size inadequate for visualization under a light microscope. These cells probably correspond to the ground-glass nuclei described in light microscopic studies as characteristic of papillary carcinoma. These kinds of cells show a large network of fine fibrils of extended chromatin, suggesting that they are in a less differentiated state and that their transcription is intense.

Perichromatin granules were found to be more abundant in the nucleus of normal follicular cells than in most carcinoma cells. Previous studies demonstrated that the frequency of these granules is low in undifferentiated cells and increases during the functional maturation that takes place in normal embryonic development [30–32]. Thus, the relative scarcity of perichromatin granules in cancer cells compared to normal cells, may be due to their lesser degree of differentiation.

The fibrillar structure surrounding the nucleolus as a halo was previously seen in papillary carcinoma cells using standard electron microscopic procedures [33]. In the present study, we demonstrate the presence of EDTA-positive fibro-granular structures in the perinucleolar space and the exclusion of other normal nuclear components. These results suggest that the nucleolar halo corresponds to altered exportation of nucleolar components.

Nuclear bodies are 1 to 1.5-μm-diameter intranuclear spherical structures found in various normal and pathological cells. They have been grouped in five different types according to their size and the distribution of their fibrillar and granular components [29]. Nuclear bodies have been found to be particularly frequent in several human diseases, including

FIG. 9 *Normal thyroid follicular cell nucleus stained by the EDTA procedure preferential for RNP. A thick layer of compact chromatin* (c) *is clear gray. RNP-containing fibrils and granules located in the interchromatin space are darkly stained. The arrows point to perichromatin granules. Bar* = 1 μm, *×16,000.*

FIG. 10 *Papillary carcinoma cell nucleus stained using the EDTA procedure. The nucleolus* (n) *manifests a large fibrillar center* (arrow). *RNP-containing fibrils and large clusters of interchromatin granules* (i) *can be seen in the nucleoplasm. Compact chromatin* (c) *forms a thin peripheral layer and a few small clumps. The nuclear body* (nb) *is formed by bleached thin fibrils and dark-stained small granules. The arrowheads point to perichromatin granules. Bar* = 1 μm, *×16,000.*

FIG. 11 *Very irregularly shaped nucleus of a papillary carcinoma cell. The nucleolus* (n) *is small and compact. The nucleoplasm contains less RNP-containing structures than the nucleus in the preceding figure. Perichromatin fibrils* (f) *can be seen in the border of some clumps of compact chromatin. The arrows point to perichromatin granules. Cy, a region of cytoplasm completely surrounded by the nucleus. Bar* = 1 μm, *×20,000.*

FIG. 12 *Nucleus of a papillary carcinoma cell stained with EDTA procedure. Fibrillar* (f) *and granular* (g) *components can be seen in the nucleolus, which presents a nucleolonemal structure. A double fibrillar layer* (fl) *surrounds the nucleolus. In the intervening zone EDTA-positive fibro-granular structures roughly radially oriented can be seen. Standard nuclear structures as compact chromatin and perichromatin and interchromatin granules are absent from this region. Bar* = 1 μm, *×32,000.*

FIG. 13 *Nucleus of a papillary carcinoma cell stained with uranyl acetate and lead citrate. Immunolabeling with anti-DNA. A large spherical nuclear body formed by an external layer of faintly stained fine fibrils irregularly oriented, an intermediate layer of DNA-containing dark fibrillar structures, and an internal layer of fibers without DNA. Bar* = 1 μm, *×33,500.*

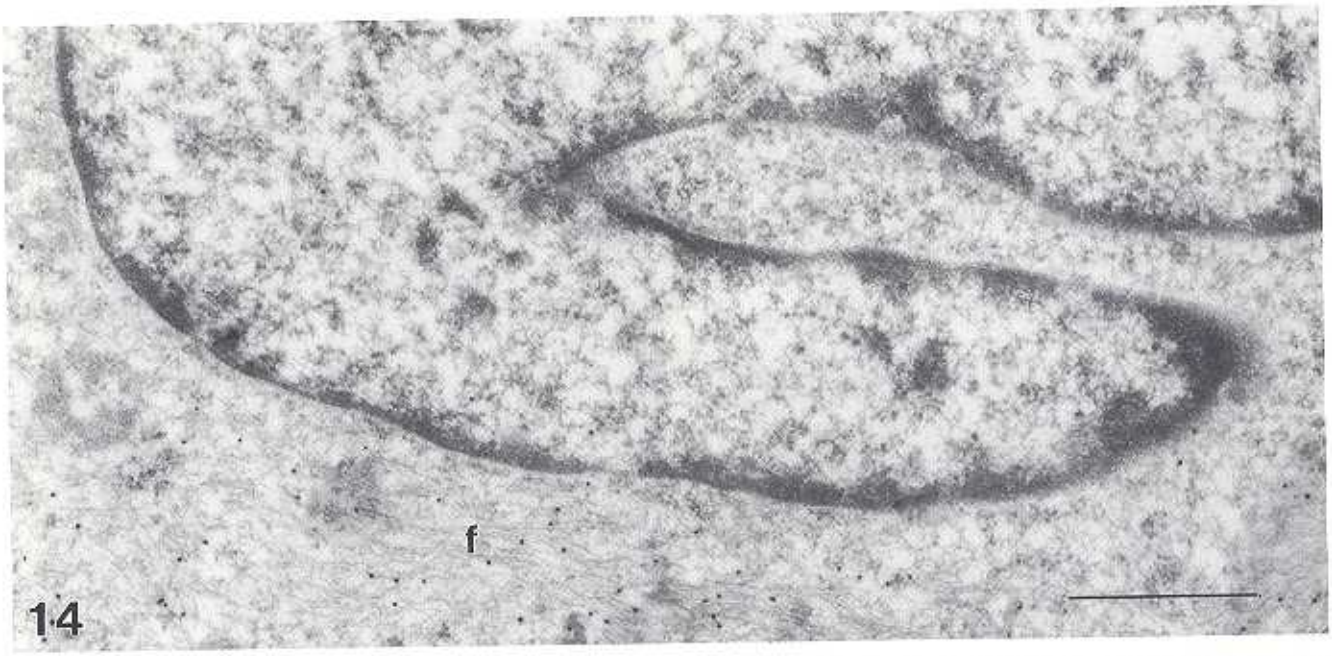

14

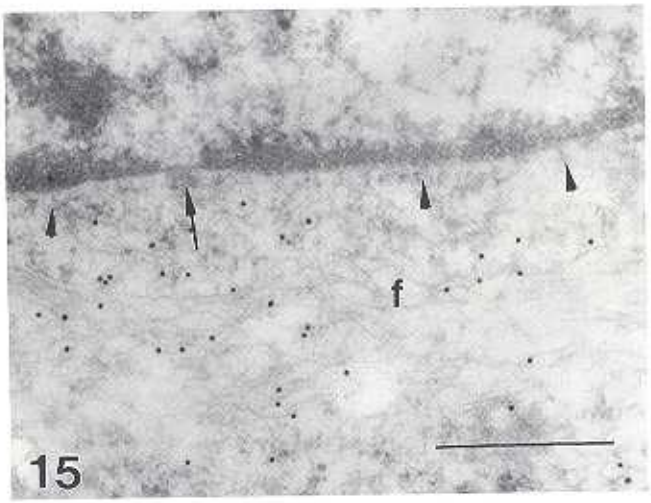

15

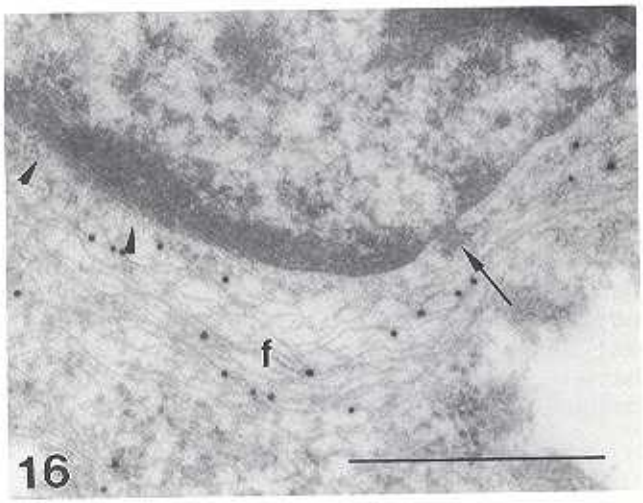

16

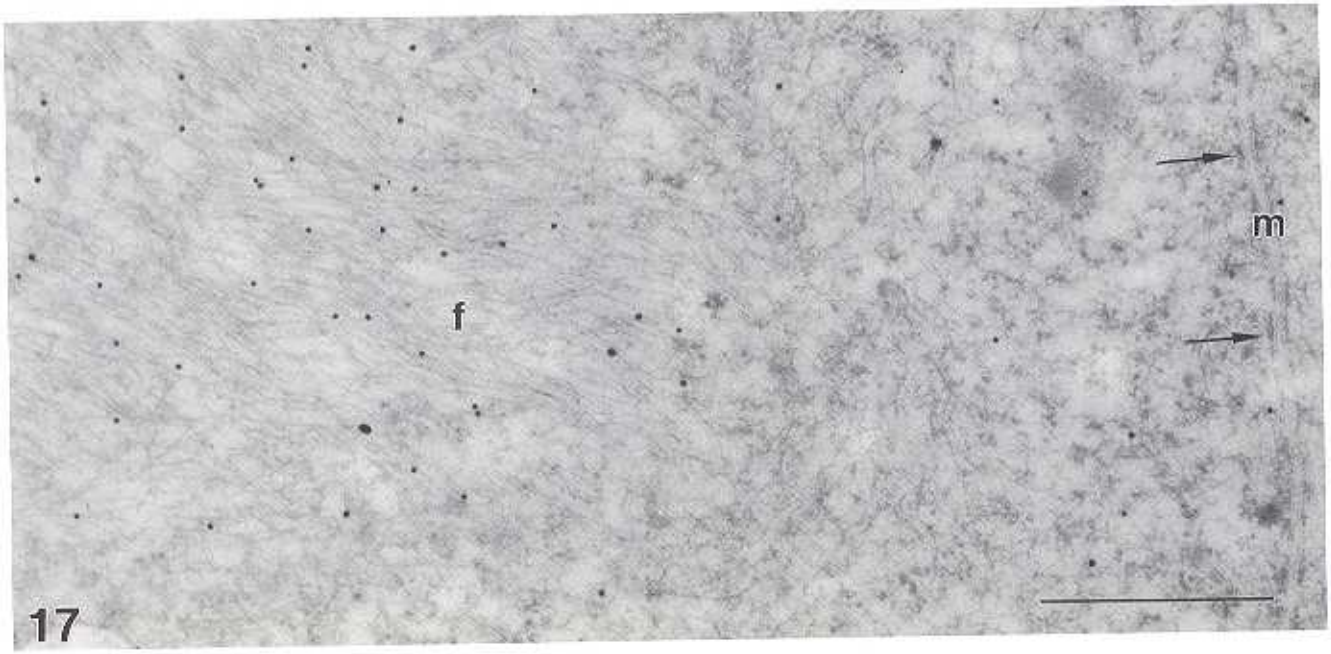

17

several carcinomas, leukemia, and viral diseases [29]. Recent biochemical and morphological studies reveal that nuclear bodies are involved in acute promyelocytic leukemia. The retinoic acid administration, which causes blast differentiation, results in the reaggregation of several antigens into the nuclear bodies [34]. In the present study nuclear bodies were found in small numbers in normal follicular cells. The frequency of nuclear bodies of the types 1, 2, and 3 is very high in carcinoma cells. Nuclear bodies of types 2 and 3 contain granules darkly stained by EDTA, similar to those in cervical carcinoma [35].

Lamins were initially identified by electron microscopy (see review in [24]), and then characterized as members of the IF superfamily by sequence analysis [36]. Lamins form a fibrous meshwork, called nuclear lamina, which is closely apposed to the nucleoplasmic surface of the inner nuclear membrane [24, 37]. It is thought to perform a skeletal function important for nuclear envelope integrity [38] and interphase chromatin organization [39], which could be also important for DNA replication and differential gene expression [40, 41]. There are three major lamins in mammals, designated as lamins A, B, and C. Lamin B is implicated in anchoring the lamina to the nuclear membrane, while lamins A and C interact with chromatin and are cross-linked in a highly discontinuous, apparently fibrillar, network that leaves large voids in the nuclear periphery [24, 37, 42]. In normal embryonic development, lamin expression is often coincident with tissue differentiation [43, 44]. The same situation has been observed in pathologic conditions like cancer. In fact, in several human and murine cancer cells lines there is no expression of lamins A and C [44, 45]. Interestingly, their expression can be induced by cellular differentiation [44].

The anti-lamin monoclonal antibody used in the present study (L3f4) recognizes an evolutionary conserved epitope present on A-type as well as on B-type lamins B1 and B2 of vertebrates [28]. The reactivity of the antibody has been reported to be restricted to the nuclear periphery by immunocytochemistry at light microscopic level and by preembedding immunoelectronmicroscopy localization [28]. The postembedding procedure employed in this study shows abundant labeling in the internal nuclear structures of normal thyroid follicular cells, and to a lesser extent in carcinoma cells. Although our results of the immunolocalization of lamins were not quantitatively analyzed, they show clear differences in the amount of labeling between normal follicular cells and papillary carcinoma cell nuclei. Normal follicular cells present higher lamin immunolabeling than papillary carcinoma cell nuclei. These results suggest that the multilobated or grooved carcinoma cell nuclei may be partially the result of a defect in the expression of nuclear lamins associated with the abnormal neoplastic cell differentiation pattern.

The cytoplasm of normal follicular cells showed scarce immunolabeling for vimentin, and none for desmin. In contrast, many papillary carcinoma cells showed cytoplasmic perinuclear bundles of filaments immunoreactive to vimentin or desmin. Thus, this IF ring around the nucleus seems to be tumor cell-specific, and may also participate in the formation of nuclear envelope invaginations. Both cytoplasmic IFs detected in the present study are organized as a dense and extended system that stretches from the nuclear envelope to the plasma membrane. Because the antibodies do not penetrate the thickness of the section and react only with epitopes exposed on its surface, all the filaments contained in the section cannot be labeled. Thus, the intermingling of vimentin and desmin filaments in the same bundles cannot be excluded and is probably frequent. The general distribution of vimentin filaments is similar to their arrangement in normal cells, except for their extreme abundance [24, 25]. However, desmin filaments are not found in normal thyroid follicular cells by means of the immunocytochemical reaction carried out in the same conditions used for papillary carcinoma cells. Desmin filaments are characteristic of muscle cells and their abundance in papillary carcinoma cells suggests that these neoplastic cells express genes that are normally transcribed in other normal differentiated cells.

Cytoplasmic IF–nuclear membrane interactions have been demonstrated in the case of vimentin, desmin, and peripherin, and they seem to be medi-

FIG. 14 *Carcinomatous cell stained with uranyl acetate and lead citrate, labeled by anti-vimentin Mab. A bundle of labeled filaments* (f) *is roughly parallel to the nuclear envelope. Bar* = 1 μm, ×31,000.

FIG. 15 *Carcinomatous cell stained and labeled as in Figure 14. Labeled filaments* (f) *form a loose network. Many of these filaments are parallel to the nuclear envelope. The arrow points to insertions of vimentin filaments to fibrils of the nuclear pore complex. Attachments to other regions of the nuclear envelope can also be seen* (arrowheads). *Bar* = 0.5 μm, ×49,500.

FIG. 16 *Carcinomatous cell stained and labeled as in Figure 14. A bundle of vimentin filaments* (f) *surrounds a portion of the nucleus. The arrowheads point to insertions of vimentin filaments to the nuclear membrane in sites not related to pore complexes. The arrow indicates fibrils of a pore complex, which shows associations with intermediate filaments. Bar* = 0.5 μm, ×77,500.

FIG. 17 *Papillary carcinoma cell labeled by anti-desmin. A large bundle of labeled filaments* (f) *is oriented in the direction of the nucleus–cell membrane* (m). *Insertions of intermediate filaments in small, paired dark-stained regions of the cell membrane, similar to desmosomes, can be seen* (arrows). *Bar* = 0.5 μm, ×50,000.

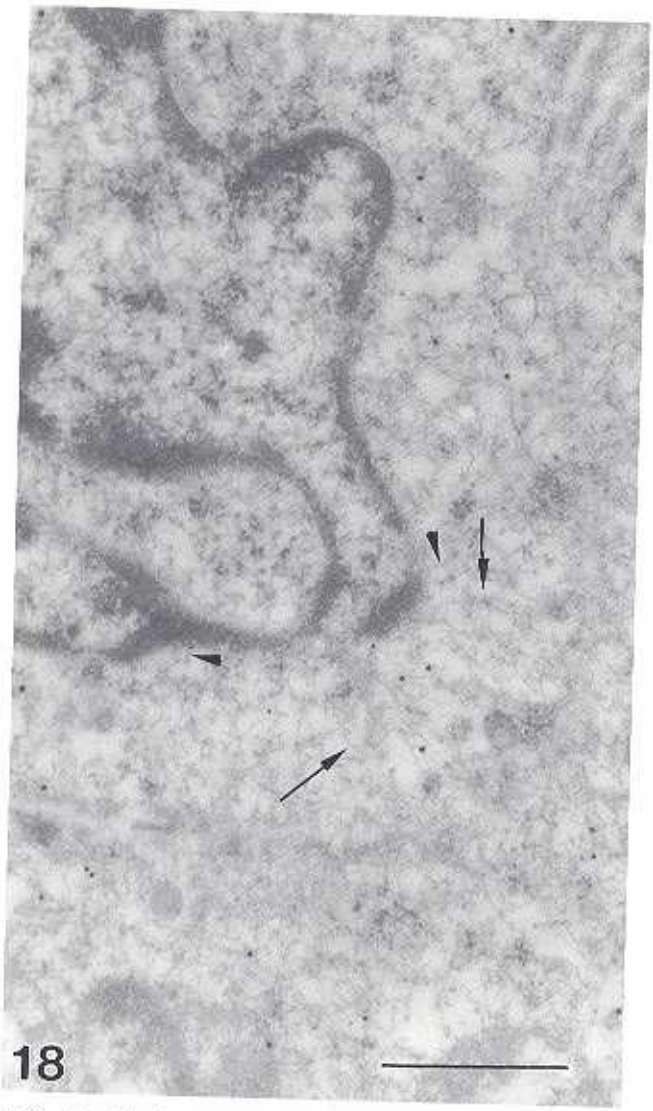

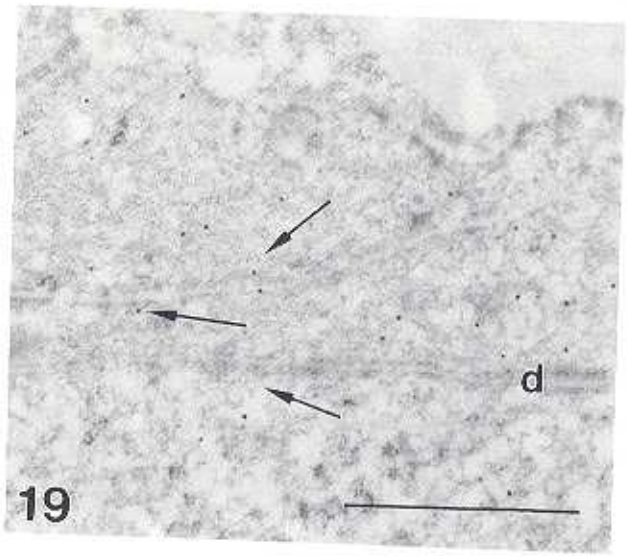

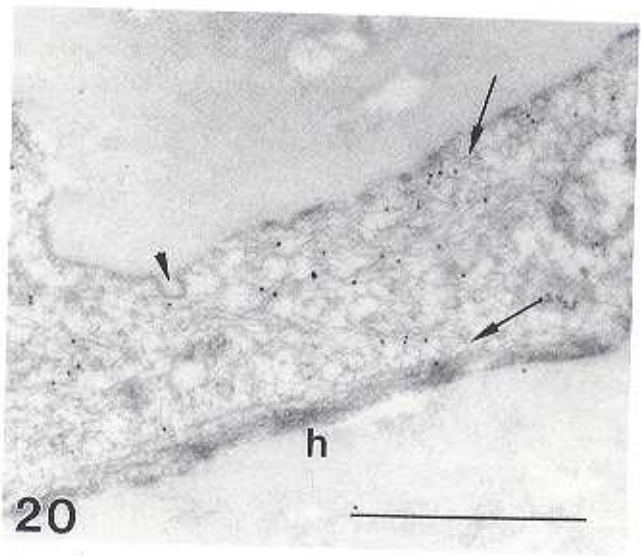

FIG. 18 *Nucleus of a papillary carcinoma cell stained with uranyl acetate and lead citrate, labeled by anti-vimentin. Labeled fibrils are arranged in a network with a predominant orientation in the direction of the nuclear envelope–cell membrane* (arrows). *Arrowheads point to insertions of vimentin filaments in the nuclear envelope not related to nuclear pore complexes. Bar* = 0.5 μm, ×47,500.

FIG. 19 *Cytoplasm of three papillary carcinoma cells stained with uranyl acetate and lead citrate. A network of anti-desmin labeled fibrils can be seen in each cell. Some fibrils of the network attach to a desmosome* (d). *More frequently the filaments connect to the cell membrane through thin, dense-stained regions not forming typical desmosomes* (arrows). *Bar* = 1 μm, ×30,000.

FIG. 20 *A digitiform protrusion of the cytoplasm of a carcinoma cell stained with uranyl acetate and lead citrate, immunolabeled with anti-vimentin. The network of filaments is intensively labeled. Two different types of attachments of filaments to the cell membrane can be seen:* (a) *Fibrils connect to thick, dense-stained regions constituting hemidesmosomes* (h), *as the cell is not in contact with other cells, but is surrounded by an extracellular matrix.* (b) *Fibrils connect to the membrane through very thin, dense-stained regions scattered on the cell membrane* (arrows). *Arrowhead, coated pit. Bar* = 1 μm, ×30,000.

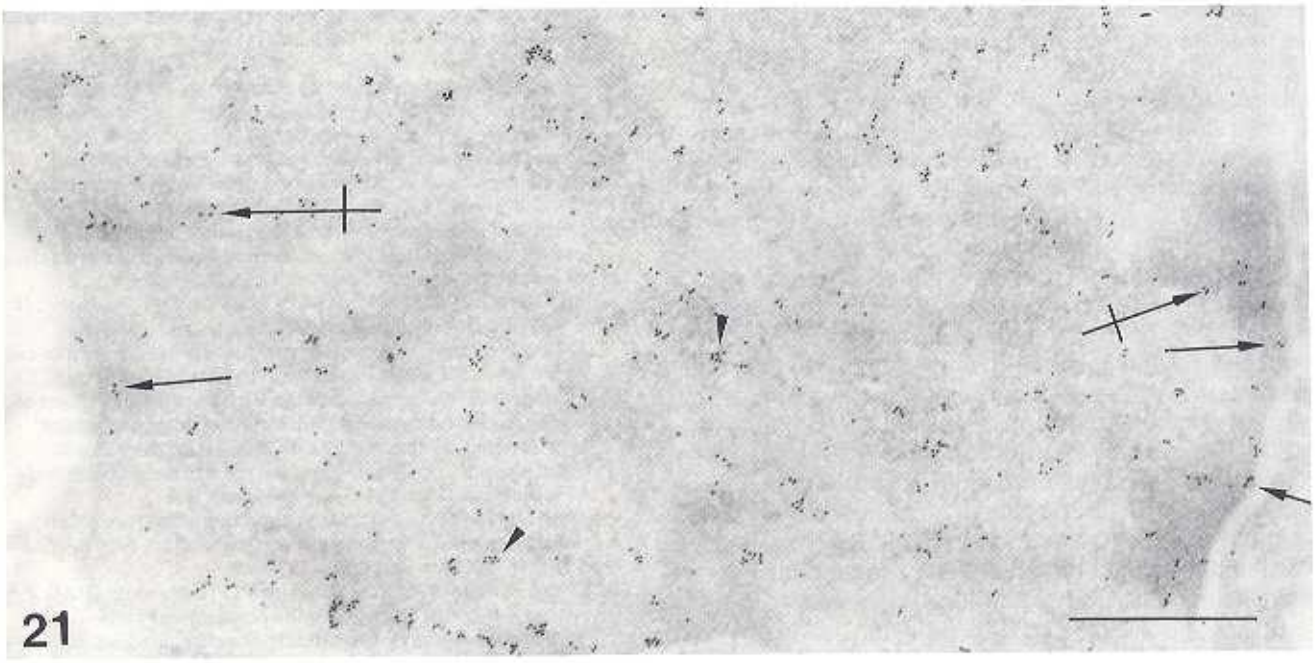

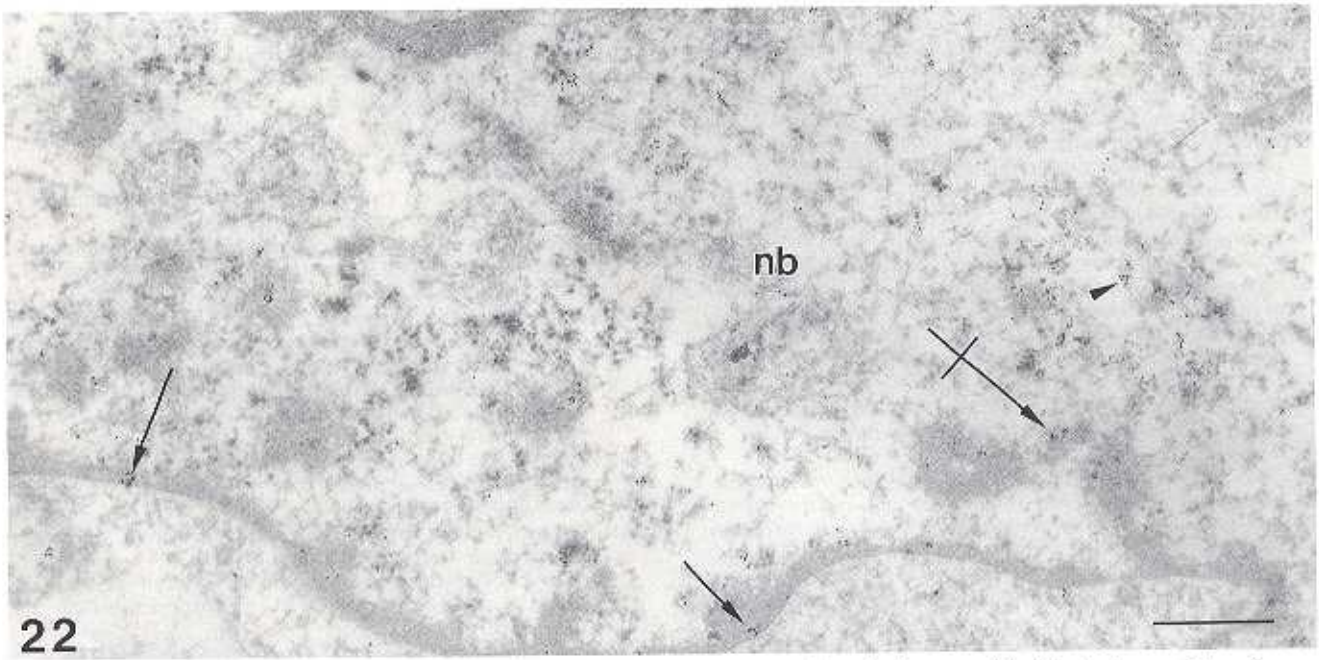

FIG. 21 *Normal follicular cell faintly stained with uranyl acetate and lead citrate to highlight the anti-lamin labeling. Gold grains are mainly located along the internal side of the nuclear envelope* (arrows), *interchromatin space* (arrowheads), *and in the periphery of compact chromatin masses* (crossed arrow). *Bar* = 0.5 μm, ×*50,000*.

FIG. 22 *Nucleus of a carcinoma cell stained and labeled as in the preceding figure. Labeling is less intense than in the normal cell nucleus. A type 1 nuclear body* (nb) *shows labeled fibrils. Arrows indicate anti-lamin labeling in contact with the nuclear envelope. The cross arrow points to gold grains in the periphery of compact chromatin clumps, and the arrowhead shows labeling in the interchromatin space. Bar* = 0.5 μm, ×*31,000*.

ated by B lamins [46]. Thus, apart for contributing to the localization of cellular organelles and the nucleus, cytoplasmic IFs also participate in support of the nuclear envelope [24, 25]. Recently, the presence of IF rings surrounding the nucleus have been demonstrated in a human pancreatic cancer cell line, uteri cervical carcinoma, melanoma, and lymphoblastic leukemia [47, 48]. In all these cancers, neoplastic cells showed nuclear lobulation, in a similar fashion to that in papillary thyroid carcinoma. Thus, it is possible that in all these situations, the nuclear envelope invaginations could be the result of external pressure produced by the thick filamentous ring, alone or in association with a defect in the nuclear lamina.

In conclusion, our results show that in papillary thyroid carcinoma cells, there are changes in the distribution of ribonucleoproteins and chromatin, in coexistence with scarce lamin immunolabeling and perinuclear vimentin and desmin filamentous rings, which alone or in conjunction may produce the characteristic multilobated and ground-glass nuclei.

REFERENCES

1. Williams ED, Doniach I, Bjarnson O, Michie R. Thyroid cancer in an iodide rich area. *Cancer*. 1997;39:215–222.
2. LiVolsi VA. Papillary neoplasms of the thyroid: pathologic and prognostic features. *Am J Clin Pathol*. 1992;97:426–432.
3. Woolner LB, Beahrs OH, Black BM. Classification and prognosis of thyroid carcinoma: a study of 885 cases observed in a thirty-year period. *Am J Surg*. 1961;102:354–387.
4. Vickery AL, Carcangiu M, Johannessen JB, Sobrinho-Simoes M. Papillary carcinoma. *Sem Diagn Pathol*. 1985;2:90–100.
5. Johannessen JV, Gould VE, Wellington J. The fine structure of human thyroid cancer. *Hum Pathol*. 1978;9:385–399.
6. Beaumont A, Ben Othman S, Fragu P. The fine structure of papillary carcinoma of the thyroid. *Histopathology*. 1981;5:377–388.
7. Chan JK, Saw D. The grooved nucleus: a useful diagnostic criterion of papillary carcinoma of the thyroid. *Am J Surg Pathol*. 1986;10:672–679.
8. Rosai J, Carcangiu ML, DeLellis RA. Papillary carcinoma. In: Rosai J, ed. *Atlas of Tumor Pathology: Tumors of the Thyroid Gland*. Washington, DC: Armed Forces Institute of Pathology; 1992:65–96.
9. Monneron A, Bernhard W. Fine structural organization of the interphase nucleus of mammalian cells. *J Ultrastruct Res*. 1969;27:266–288.
10. Fakan S, Puvion E. The ultrastructural localisation of nucleolar and extranucleolar RNA synthesis and distribution. *Int Rev Cytol*. 1980;65:255–299.
11. Puvion E, Moyne G. In situ localisation of RNA structure. In: Busch H, ed. *The Cell Nucleus*. New York: Academic; 1981;8:59–115.
12. Bachellerie JP, Puvion E, Zalta JP. Ultrastructural organization and biochemical characterization of chromatin RNA–protein complexes isolated from mammalian cell nuclei. *J Microsc*. 1975;126:77–85.
13. Fakan S, Puvion E, Spohr G. Localisation and characterization of newly synthesized nuclear RNA in isolated hepatocytes. *Exp Cell Res*. 1976;99:155–164.
14. Fakan S, Leser G, Martin T. Ultrastructural distribution of nuclear ribonucleoproteins as visualized by immunocytochemistry in thin sections. *J Cell Biol*. 1984;98:358–363.
15. Fakan S, Leser G, Martin T. Immunoelectron microscope visualization of nuclear antigens within spread transcription complexes. *J Cell Biol*. 1986;103:1153–1157.
16. Vàzquez-Nin GH, Bernard W. Comparative ultrastructural study of perichromatin and Balbiani ring granules. *J Ultrastruct Res*. 1971;36:842–860.
17. Vázquez-Nin GH, Echeverría OM, Fakan S, Leser G, Martin T. Immunoelectron microscope localization of snRNPs in the polytene nucleus of salivary glands of *Chironomus thummi*. *Chromosoma*. 1990;99:44–51.
18. Vázquez-Nin GH, Echeverría OM, Pedron J. Effects of estradiol on the ribonucleoprotein constituents of the nucleus of cultured endometrial epithelial cells. *Biol Cell*. 1979;35:221–228.
19. Echeverría OM, Zavala G, Benitez A, Vázquez-Nin GH. Changes during estral cycle in the nucleus of endometrial cells of the rat. *Biol Cell*. 1980;39:139–142.
20. Echeverría OM, Pagán-Santini R, Vázquez-Nin GH. Effect of testosterone on nuclear ribonucleoprotein components of prostate epithelial cells. *Biol Cell*. 1991;72:223–229.
21. Vázquez-Nin GH, Ortega-Rangel JA, Echeverría OM, Parra MR, Jiménez-García LF. Changes in nuclear ribonucleoprotein constituents and chromatin disposition during neuronal differentiation and maturation. *Biol Cell*. 1983;48:17–24.
22. Zavala G, Aguilar X, Jiménez-García LF, Echeverría OM, Vázquez-Nin GH. Changes in the ribonucleoprotein constituents of the nucleus during the differentiation of muscle cells in the chick embryo. *Biol Cell*. 1992;76:159–165.
23. González-Oliver A, Echeverría OM, Hernández-Pando R, Vázquez-Nin GH. Ultrastructural study of the nuclei of normal, dysplastic and carcinomatous epithelial cells of the human cervix uteri. *Ultrastruct Pathol*. 1997;21:379–392.
24. Fuchs E, Weber K. Intermediate filaments: structure, dynamics, function and disease. *Annu Rev Biochem*. 1994;63:345–382.
25. Alberts B, Bray D, Lewis J, Raff M, Roberts K, Watson JD. *Molecular Biology of the Cell*. New York: Garland; 1989:613–680.
26. Bernhard W. A new procedure for electron microscopical cytology. *J Ultrastruct Res*. 1969;27:250–265.
27. Vázquez-Nin GH, Chávez B, Tomàs-Martin C. A preferential method for chromatin in electron microscopy. *J Microsc*. 1973;16:243–246.
28. Vester B, Smith A, Krohne G, Benavente R. Presence of a nuclear lamina in pachytene spermatocytes of the rat. *J Cell Sci*. 1993;104:557–563.
29. Bouteille M, Kalifat R, Delarue J. Ultrastructural variations of nuclear bodies in human diseases. *J Ultrastruct Res*. 1967;19:474–486.
30. Vázquez-Nin GH, Ortega-Rangel JA, Echeverría OM. Nuclear aspects of neuroblast differentiation in the chick embryo. *Biol Cell*. 1980;39:143–146.
31. Vázquez-Nin GH, Ortega-Rangel JA, Echeverría OM, Parra MR, Jiménez-García LF. Changes in nuclear ribonucleoprotein constituents and chromatin disposition during neuronal differentiation and maturation. *Biol Cell*. 1983;48:17–24.
32. Zavala G, Aguilar X, Jiménez-García LF, Echeverría OM, Vázquez-Nin GH. Changes in the ribonucleoprotein constituents of the nucleus during the differentiation of muscle cells in the chick embryo. *Biol Cell*. 1992;76:159–165.
33. Beaumont A, Ben Othman S, Fragu P. The fine structure of papillary carcinoma of the thyroid. *Histopathology*. 1981;5:377–388.
34. Kokan MHM, Puvion-Dutilleul F, Guillermin MC, et al. The t(15;17) translocation alters a nuclear body in a retinoic acid-reversible fashion. *EMBO J*. 1994;13:1073–1083.
35. González Oliver A, Echeverría OM, Hernández Pando R, Vázquez-Nin GH. Ultrastructural study of the nuclei of normal, dysplastic, and carcinomatous cells of the human cervix uteri. *Ultrastruct Pathol*. 1997;21:379–392.
36. Fisher DZ, Chaudhary N, Blobel G. cDNA sequencing of nuclear lamins A and C reveals primary and secondary structural homology to intermediate filament proteins. *Proc Natl Acad Sci*. 1986;83:6450–6454.

37. Gerace L, Comeau C, Benson M. Organization and modulation of nuclear lamina structure. *J Cell Sci*. 1984;(suppl 1):137–160.
38. Gerace L, Blobel G. The nuclear envelope lamina is reversibly depolymerized during mitosis. *Cell*. 1980;19:277–287.
39. Benavente R, Krohne G. Involvement of nuclear lamins in postmitotic reorganization of chromatin as demonstrated by microinjection of lamin antibodies. *Cell*. 1986;103:1847–1854.
40. Hancock R. Topological organization of interphase DNA: the nuclear matrix and other skeletal structures. *Biol Cell*. 1982;46:105–122.
41. Hozák P, Hassan B, Jackson DA, Cook P. Visualization of replication factories attached to a nucleoskeleton. *Cell*. 1993;73:361–373.
42. Paddy M, Belmont A, Saumweber H, Agard D, Sedat J. Interphase nuclear envelope lamins form a discontinuous network that interacts with only a fraction of the chromatin in the nuclear periphery. *Cell*. 1990;62:89–106.
43. Lehner C, Stick R, Eppenberger H, Nigg E. Differential expression of nuclear lamin proteins during chicken development. *J Cell Biol*. 1987;105:577–587.
44. Röber R, Weber K, Osborn M. Differential timing of nuclear lamin A/C expression in the various organs of the mouse embryo and the young animal: a developmental study. *Development*. 1989;105:365–378.
45. Guilly M, Bensussan A, Bourge J, Bornens M, Courvalin J. A human T lymphoblastic cell line lacks lamins A and C. *EMBO J*. 1987;12:3795–3799.
46. Georgatos SD, Blobel G. Lamin B constitutes an intermediate filament attachment site at the nuclear envelope. *J Cell Biol*. 1987;105:117–125.
47. Kamei H. Relationship of nuclear invaginations to perinuclear rings composed of intermediate filaments in MIA PaCa-2 and some other cells. *Cell Structure and Function*. 1994;19:123–132.
48. Slater L, Sweet P, Hsu TC, Chan PK. Novel nucleolar and nuclear morphology in a vincristine-dependent human leukemia cell line (L 100). *Exp Cell Res*. 1992;198:170–174.